

# Fourier Methods for Noisy and Chaotic Systems

Jonah Sachs<sup>1</sup> and Leshan Yang<sup>1</sup>

<sup>1</sup>*Department of Physics, Washington University, St. Louis, Missouri 63130*

(Dated: December 10, 2024)

The Fourier Transform is a mathematical tool that breaks a complex-valued function down into its constituent frequencies. The Fast Fourier Transform (FFT), is a popular evolution of the Fourier Transform which calculates the Discrete Fourier Transform (DFT) of a discrete series of  $n$  values [1]. Use of the FFT has allowed scientists to analyze the frequency domain with higher accuracy, allowing for refined signal analysis by revealing periodic components in the presence of electronic noise and complex signal combinations. The FFT reduces the Fourier Transform's runtime from  $O(n^2)$  to  $O(n\log n)$ , allowing for the processing of larger  $n$ . Spectrum/Network analyzers use the FFT to reveal information about the frequency domain in real-time [2]. Scientists, engineers, and technicians alike utilize network analyzers to process information from noisy or complicated patterns in data. This experiment will demonstrate the use of a network analyzer, and the FFT, in different disciplines. Results demonstrate the tool's ability to reveal periodic information in a variety of signal-processing use cases. This ability extends to signals with very small amplitude, despite our setup including only basic electrical lab equipment and materials.

## INTRODUCTION

Any periodic function, with period  $T$ , can be decomposed into the sum of sine and cosine components of varying frequencies. This is the premise behind the Fourier series of a function. Mathematically, this is defined as [3]:

$$g(t) = \frac{a_0}{2} + \sum_{n=1}^{\infty} \left\{ a_n \cos\left(\frac{2\pi nt}{T}\right) + b_n \sin\left(\frac{2\pi nt}{T}\right) \right\}. \quad (1)$$

In the context of signal analysis,  $\frac{a_0}{2}$  represents the DC offset, compared to the oscillatory AC components to be decomposed in the Fourier spectrum.  $a_n$  and  $b_n$  are the coefficients associated with the sine and cosine components of different frequencies. The fundamental frequency of the first harmonic is determined by the period  $T$ . We define it:  $\nu_0 = 1/T$ . We also define as the spacing between frequency components:  $\Delta f = \nu_0 = 1/T$ .

As we apply the limit of  $T \Rightarrow \infty$ , we are left with the following expression [3], commonly known as the Fourier transform of any integrable function  $f(t)$ :

$$F(\omega) = \int_{-\infty}^{\infty} f(t) e^{-i\omega t} \quad \omega = 2\pi f. \quad (2)$$

For discretized data, we have to transition our expression to accommodate a series of individual data points. We can define the Discrete Fourier Transform (DFT) as follows [3]:

$$\tilde{G}_n = \sum_{k=0}^{N-1} g_k e^{-i2\pi \frac{k}{N} n}. \quad (3)$$

Where we define  $N$  sampling points. For a window size  $T$ , the sample spacing  $\Delta t = \frac{T}{N}$ . We know that any data

point occurs at  $t_k = \frac{kT}{N}$ , and that  $g_k = g(\frac{kT}{N})$ . The fundamental frequency is still  $\nu_0 = \frac{1}{T} = \frac{1}{N\Delta t}$ , with an equivalent frequency spacing  $\Delta f = \frac{1}{N\Delta t}$ .

Assuming we are taking the same amount of data points, this gives a fundamental inverse relationship between  $\Delta f$  and  $\Delta t$ . Creating finer data in the frequency domain creates less fine data in the time domain, and vice versa.

As we will orchestrate throughout this paper, the conversion from time series components to frequency-series components is often useful to various applications in signal processing. This conversion will occur throughout a device known as a Network Analyzer (NA), which runs and displays the coefficients of the DFT of an input signal in real-time. The specific NA to be used is the Model SR770 FFT Network Analyzer from Stanford Research Systems [4]. This machine has many customizable features to aid in signal processing, its use will be displayed throughout this study.

## METHODS

Signal processing over the course of the experiment utilized various general electrical components, which will be described here. The oscilloscope is a device used for displaying signals in the time domain. The SR770 FFT Network Analyzer (SR770) was used for displaying signals in the frequency domain. The Signal Generator was used for generating an external signal with specific waveform parameters such as the frequency and amplitude.

In addition, the Fourier Methods Electronic Modules (FMEM) is a device provided by TeachSpin which includes inbuilt electrical equipment. Used were the following sections of the FMEM, which can be modulated together: a filter unit with options for low-pass, high-pass, and band-pass filters, a wide-band amplifier for

amplifying signals over a large bandwidth, summer and multiplier units for inbuilt signal math, a power audio amplifier unit and speaker unit for audio testing, and a DC offset for providing a DC current. There are also the chaos and buried treasure units of the FMEM, which are used for core experiments, and will be further discussed later in this study.

## SIGNAL DETECTION

What are the advantages of the frequency domain, and why do we need a device like the SR770? Consider the waveform like that provided in Figure 1.

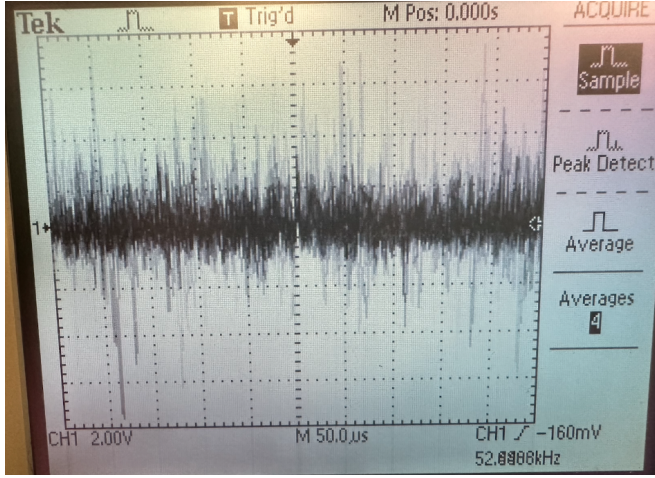


FIG. 1: Buried signal A in time domain on the Oscilloscope

It may not seem like it, but buried underneath all those fluctuations (or noise) is a sinusoidal waveform. In the time domain, it is impossible to discern. The same is not true for a noisy signal like the one presented, when analyzed in the frequency domain.

Consider Figure 2, which offers a look into the frequency domain. We see signal D, which possesses a much smaller amplitude than signal A, clearly removable and discernible.

For a sample with a smaller amplitude, we simply have to decrease the size of the frequency span for higher accuracy. For example, as we decrease the span from 100 kHz to 6.25 kHz, the acquisition time on the SR770 increases from 4 ms to 64 ms [2]. This relationship was described generally earlier. With this method, signals with extremely small amplitude can be found, given you have the time to search through enough intervals.

Figure 2 offers some insights into the usefulness of the frequency domain in signal analysis. Given a large averaging sample, we can easily pick out even a small sinusoidal amplitude for a correctly chosen span. This is because electronic noise will average to zero across the

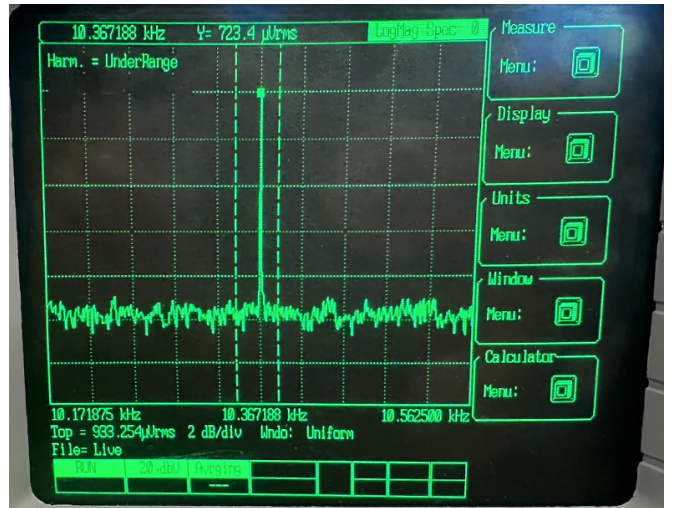


FIG. 2: Buried signal D in frequency domain on the SR770

full bandwidth, but the sinusoidal signal will not [2].

In addition to signal detection, the SR770 also aids in signal analysis. In the top left of Figure 2, clearly revealed in the resonant frequency of the sinusoidal waveform. Given some further calculations, the SR770 can also be used for determining the amplitude of the waveform. We start with the following equation:

$$\langle [V_n(t) + A \cos(\omega t - \phi)]^2 \rangle = S\delta f + \frac{A^2}{2} \quad (4)$$

Where  $V_n(t)$  is the noise's voltage function and  $A \cos(\omega t - \phi)$  is the voltage function of the signal buried underneath the noise. This form is taken from the general form for a harmonic.  $\delta f$  is the equivalent bandwidth, or the bandwidth for an ideal filter system approximated from our non-ideal filter system.

Our goal is to determine  $\langle V_n^2 \rangle$  and  $\langle V_{tot}^2 \rangle$ . Since the noise is linearly separable, we can then easily subtract for  $\langle V_{sig}^2 \rangle$  given these values, and determine the amplitude  $A$  [2]. To determine  $\langle V_n^2 \rangle$ , we turn our attention to the noise floor. We set the SR770 to Power Spectral Density (PSD) with units Volts RMS, which returns units of  $\frac{\text{Vrms}}{\sqrt{\text{Hz}}}$ . Squaring this value returns  $S$ , the noise density. We can then calculate  $\delta f$  by dividing the span by the number of data points (400). Combining, we derive a value for  $\langle V_n^2 \rangle$ .

For  $\langle V_{tot}^2 \rangle$ , we turn our attention to the signal peak. The SR770 mode is switched to Spectrum, and the units are set to Volts Pk. This will return  $\langle V_{tot}^2 \rangle$  in units Vrms. Given this and  $\langle V_n^2 \rangle$ , we can easily solve for  $A$ .

These processes were conducted across multiple examples included in the buried treasure unit of the FMEM, with the results provided in Table I. Included are the mode used and the found frequency and amplitude.

Settings	Frequency (kHz)	Amplitude (mV)
A	2.875	11.78
B	70.25	5.77
C	33.57	1.8
D	10.37	0.96

TABLE I: Frequency and Amplitude for each setting of buried treasure

### LORENTZ ATTRACTOR

The SR770, and correspondingly the FFT, have use cases past the simple case of a noisy sinusoidal waveform. For this section of the study, we consider the case of the Lorentz Attractor.

The Lorentz Attractor was derived from an idealized version of a problem from fluid mechanics. The problem details a horizontal layer of fluid in contact with a hotter surface above and a cooler surface below. For small enough temperature deltas, this fluid can stay at rest and transfer heat from the bottom to the top purely via conduction. For a large enough difference, motion can occur. In the 2D idealization of this problem, the first mode of convection is a series of 'unit cells.' Each of these cells contains an ascending column of heated fluid that cools the top layer and descends into falling columns of fluid. These unit cells can be approximated as  $x(t), y(t), z(t)$ , where  $x(t)$  is the measure of fluid rotation in each cell,  $y(t)$  is the temperature difference between the rising and falling columns of fluid, and  $z(t)$  is a measure of the deviation from pure conduction [2]. We define the Lorentz Attractor mathematically as an Initial-Value Problem (IVP) solved by the set of first-order differential equations given below [2]:

$$\begin{aligned} \frac{dx}{dt} &= s[-x(t) + y(t)] \\ \frac{dy}{dt} &= rx(t) - y(t) - x(t)z(t) \\ \frac{dz}{dt} &= x(t)y(t) - bz(t) \end{aligned}$$

Inside the FMEM, included within the chaos module, there are three voltage outputs which mimic the behavior of these differential equations. We define  $s = 10$  and  $b = 8/3$  by convention.  $r$  is our control parameter, which can be modified by a dial included in the chaos module. This system behaves deterministically: given a set of initial conditions, the system will evolve in a singular way.

Given a specific choice of  $r$ , this system can become chaotic. In a chaotic regime, small deviations in initial conditions will cause drastically different function behavior. As a result, functions become extremely unpredictable given some experimental error. In this section,

we will vary  $r$  in an attempt to realize different regions of behavior for the Lorentz Attractor. In the process, the oscilloscope and SR770 will be used for time and frequency domain analysis respectively.

For all  $r \in (0, 1)$ , all  $x, y, z \Rightarrow 0$ . This is known as the conductive regime. Heat can be passed without any rotation of the fluid; there is no movement.

For all  $r \in (1, 25)$ , all  $x, y, z \Rightarrow$  analytically-solvable steady state values. This is the steady convection regime, where after initial transients die away, the system will settle into either clockwise or counterclockwise rotation with a steady angular velocity, steady temperature difference, and a steady (but nonzero) conduction profile.

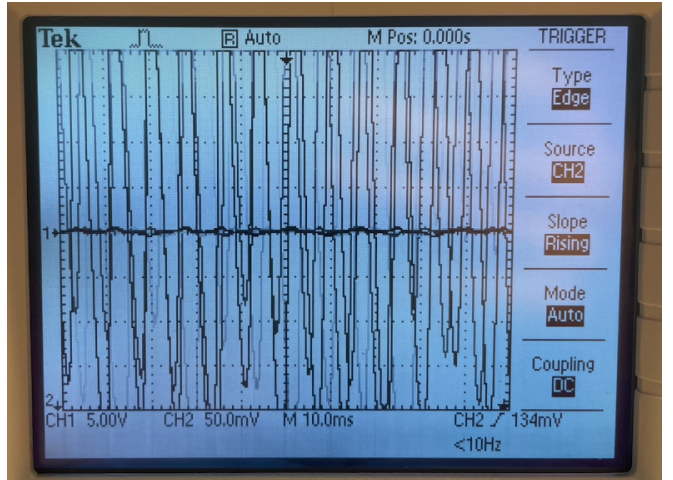


FIG. 3: Chaos found in the Y-T frame, where  $Y$  is  $y(t)$  and  $T$  is time

For  $r \geq 25$ , we see the voltage functions start to dramatically flip in sign. Past  $r = 28$ , we start to witness chaotic behavior. Given is the case for  $r = 35$ , shown in the time domain (Figure 3). For this experiment, the  $z(t)$  output was attached to both the oscilloscope and the SR770. For the oscilloscope a Y-T frame was used first, shown in Figure 3. Nothing discernible can be gained from what is clearly a chaotic plot.

Figure 4 shows an X-Y plot, also on the oscilloscope, where X is  $x(t)$  and Y is  $z(t)$ . For this case, the tuning parameter selected was  $r = 30$ . Clearly visible is the expected type of pattern for the Lorentz Attractor when undergoing chaos [2]. However, the view within the time domain does not provide us with any information about the system.

How does the SR770 factor in? We can analyze the transient behavior immediately before the chaotic regime, and gain information about the system in the process. This requires a specific choice of trigger, or the cusp of voltage at which these devices activate. For this experiment, we fed  $z(t)$  into both the oscilloscope and the SR770 as the trigger. We used  $M = 10$  ms as our sweep time to ensure the maximum amount of transient

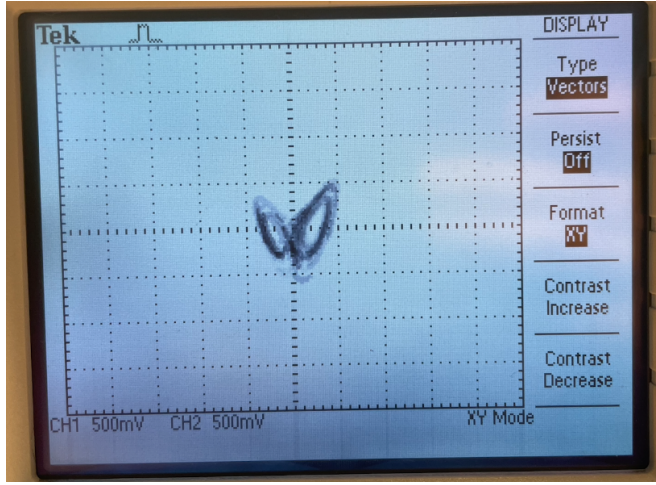


FIG. 4: Chaos found in the X–Y frame, where X is  $x(t)$  and Y is  $z(t)$

visualization before the descent into chaos. We were then able to measure the frequency of the transient wave, and could equivalently find that value on the SR770. With this information, we can solve the transient's frequency and calculate its amplitude as seen in Signal Detection.

Figure 5 displays the SR770's analysis of the transient wave, with a frequency of 153 Hz found. This was within 10 Hz of what was predicted by the oscilloscope. Not included is the visualization of the transient wave on the oscilloscope, which takes the form of a simple sinusoidal waveform.

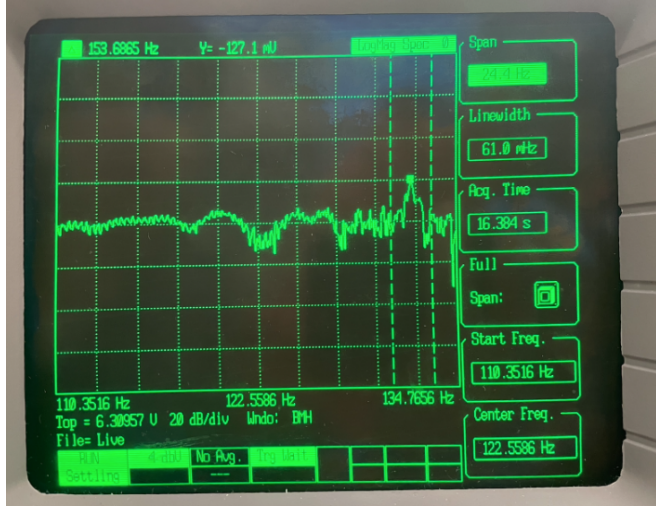


FIG. 5: Transient wave on SR770

But what about when we increase our tuning value long into the chaotic regime? The Lorentz Attractor also contains a property known as period doubling, which can be displayed with the SR770.

As we keep increasing  $r$ , the Lorentz Attractor falls

back into a steady state. This cusp occurred at  $r = 135$ . After this cusp, our function will once again display periodic behavior. Figure 9 in the Supplementary section shows this periodic behavior, displayed on the oscilloscope. We note that the periodic behavior is not readily visible on the oscilloscope. However, on the SR770, we can clearly visualize the distinct peaks in frequency.

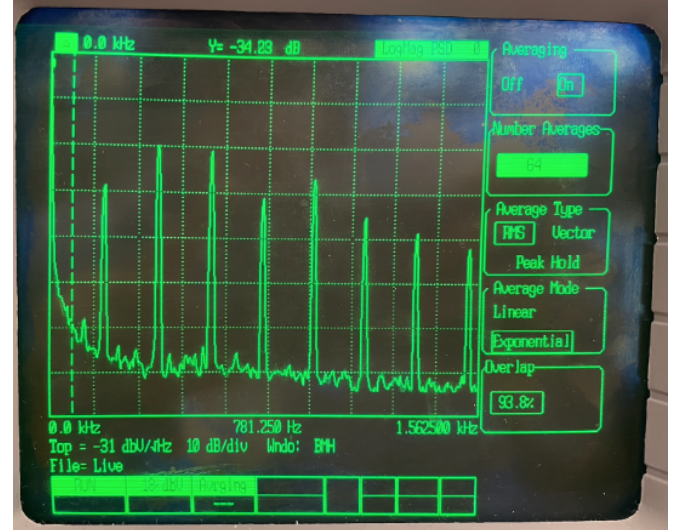


FIG. 6: SR770 view at  $r = 135$

In Figure 6, we see the periodic peaks elevated above the noise floor. We see that the peaks repeat at the multiple fundamental frequencies. These fundamental frequencies can be measured by the SR770. The amplitudes can also be calculated via the processes detailed in Signal Detection. As a result, we obtain more information about the Lorentz attractor in the frequency domain than in the time domain.

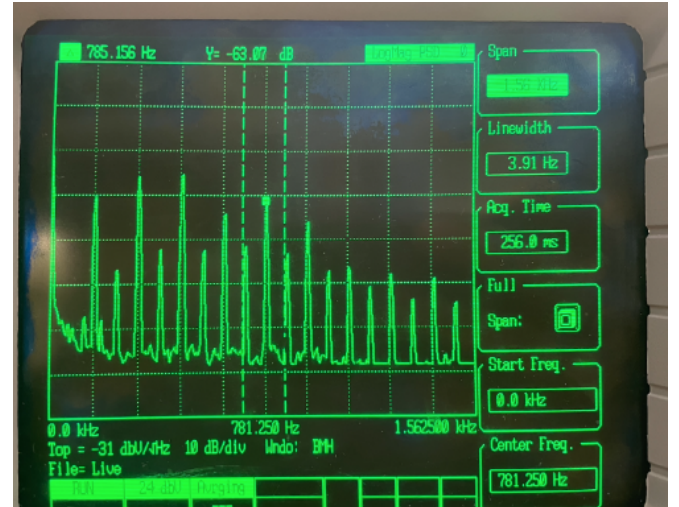


FIG. 7: SR770 view at  $r = 140$

In Figure 7, we see the effects of period doubling. Pe-

riod doubling means that we see peaks at not only the multiples of the fundamental frequencies, but we also see peaks at the multiples of half of the fundamental frequencies. This effect can clearly be illustrated when comparing Figure 6 and Figure 7.

In addition, we see that as we increase  $r$ , the period doubling pattern continues. In Figure 8, we see period quadrupling at  $r = 142$ . The time domain view of both  $r = 140$  and  $r = 142$  are shown in the Supplementary section (Figure ??, Figure ??).

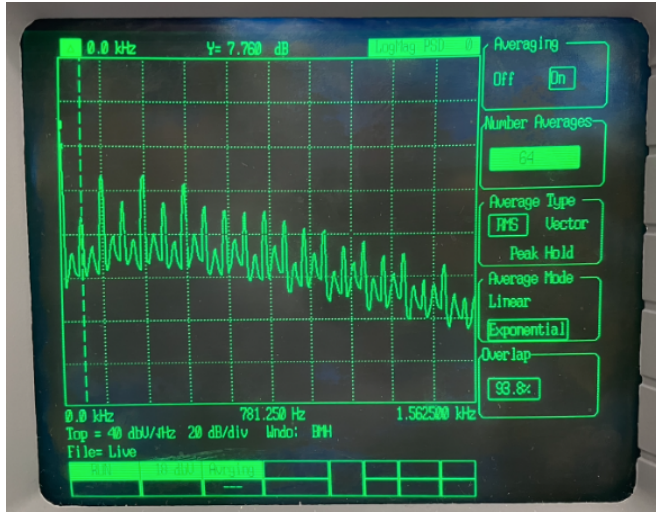


FIG. 8: SR770 view at  $r = 142$

The transition from stable periodic behavior through period doubling to chaos provides insight into the predictability and sensitivity of dynamical systems to initial conditions. As the period doubles, each new cycle becomes more complex, and small changes in the initial conditions result in significantly different trajectories, leading up to fully chaotic behavior. This explains why chaotic systems are inherently difficult to predict even though they follow deterministic laws. It also shows that there are indeed patterns within chaos.

Varying the  $r$  parameter allowed us to explore different regimes of the Lorentz Attractor. Using the SR770 and the oscilloscope, we were able to discern information about the periodic nature of these regimes. In addition, we were clearly able to display transient behavior and the nature of period doubling, which is one of the foundations of chaos theory.

Provided to the right is a table showing the notable crossover points involving  $r$ . This is intended as a helper for the reader to keep track of the values of  $r$  required for different regimes.

$r$	Description
1	Conductive to Steady Convection
25	Steady Convection to Sign-Flipping
28	Sign-Flipping to Chaos
135	Chaos to Steady State
140	Period Doubling
142	Period Quadrupling
145	Chaos

TABLE II:  $r$  values for crossover points for domains of the Lorentz Attractor

## DISCUSSION

We encountered some general errors while testing our equipment. Firstly, we noticed that the value of the noise floor, when observing specific signals buried under noise, was about two times as high as the expected value listed in the lab manual. We suspect that the internal resistance of the buried treasure module might be slightly compromised. This could potentially lead to incorrect calculations listed in Table I.

Secondly, we noticed a significant “peak to peak” value in the oscilloscope, despite not being plugged into everything. We suspected that it was the confounding variables that existed in the lab environment. We kept this in mind while comparing our values to those expected in the lab manual during the calibration of the equipment.

## CONCLUSION

In this paper, we explored the different ways we can utilize the Fourier Transform to solve difficult problems that cannot be solved in the time domain, in the frequency domain. We were able to locate very weak signals under significant noise and explore the chaos the Lorentz Attractor brings.

We found quite significant errors as we explored our equipment. However, they are most likely due to internal designs of the equipment.

## ACKNOWLEDGMENT

Special Thanks to Dr. Dong Li, Department of Physics, Washington University in St. Louis, for the advice in carrying out the experiment, as well as for helpful discussion.

**REFERENCES**

- 
- [1] B. Heideman, Johnson, *A history of the fast fourier transform* (1984), accessed: 2024-10-27, URL [https://www.cis.rit.edu/class/simg716/Gauss\\_History\\_FFT.pdf](https://www.cis.rit.edu/class/simg716/Gauss_History_FFT.pdf).
  - [2] D. V. Baak, J. Reichert, and G. Herold, *Fourier methods*,
  - TeachSpin Experimental Package (2015), URL <https://www.teachspin.com/>.
  - [3] P. 322, *smh Fourier Notes* (2014), URL <https://web.physics.wustl.edu/classinfo/322/Secure/Experiments/Physics/FourierMethods/fourier9.pdf>.
  - [4] S. R. Systems, *User's Manual Model SR770 FFT Network Analyzer* (2006), URL <https://web.physics.wustl.edu/classinfo/322/Secure/Experiments/Physics/FourierMethods/SR770Manual.pdf>.